

See discussions, stats, and author profiles for this publication at: <https://www.researchgate.net/publication/231170876>

Control of partitioning in polymer modified electrodes imposed by chemical cross-linking, for the simultaneous measurement of normally interfering analytes

ARTICLE *in* ANALYTICAL CHEMISTRY · APRIL 1993

Impact Factor: 5.64 · DOI: 10.1021/ac00071a015

CITATIONS

10

READS

21

2 AUTHORS, INCLUDING:



Johannes G Vos

Dublin City University

303 PUBLICATIONS 7,152 CITATIONS

SEE PROFILE

Control of Partitioning in Polymer Modified Electrodes Imposed by Chemical Cross-Linking, for the Simultaneous Measurement of Normally Interfering Analytes

Andrew P. Doherty and Johannes G. Vos*

School of Chemical Sciences, Dublin City University, Dublin 9, Ireland

The redox polymer $[\text{Os}(\text{bipy})_2(\text{PVP})_{10}\text{Cl}]\text{Cl}$ has been chemically cross-linked with *p*-dibromobenzene, 1,5-dibromopentane, and 1,10-dibromodecane from 1 to 20 mol % [bipy = 2,2'-bipyridyl, PVP = poly(4-vinylpyridine)]. The general electrochemistry, charge transport characteristics, and catalytic behavior of the material has been assessed. Cross-linking has a minimal effect on the general electrochemistry of the redox centers. However, partitioning of $[\text{Fe}(\text{III})]$ was physically prevented by use of 1,5-dibromopentane and 1,10-dibromodecane while reduced partitioning was evident for *p*-dibromobenzene cross-linked films, whereas the mediated reduction of NO_2^- was found to occur throughout the cross-linked polymer film. The possibility of using the different partition of these two analytes into the cross-linked polymers to simultaneously determine their concentration is demonstrated.

INTRODUCTION

Sensors based on modified electrodes have been the subject of active investigation recently, in particular those modified with electroactive polymers.¹⁻³ It has been pointed out that the electrochemical behavior observed for modified electrodes does not always agree with the general theories for mass and charge transport.⁴ To better understand these systems, attempts have been made to produce redox materials with well-behaved electrochemical properties for investigation of the mass and charge transport processes with respect to the developed theories.⁵ In this laboratory, a series of redox polymers has been developed, e.g., $[\text{Os}(\text{bipy})_2(\text{PVP})_n\text{Cl}]\text{Cl}$ (where $n = 5, 10, 15, 25$), with near-ideal electrochemical behavior.^{6,7} These materials have been shown to be effective electrocatalysts for the mediated electrocatalytic oxidation or reduction of substrates such as $\text{Fe}(\text{III})$, $\text{Fe}(\text{II})$, and NO_2^- .⁸⁻¹⁰ The electrocatalytic behavior of the materials has also been found to conform well to the general theories of mediated electrocatalysis proposed by Alberly and Hillman¹¹ and

Andrieux et al.¹² In addition, good agreement between electrocatalytic behavior and theory is evident in the environment of thin-layer flow cells.¹³ Formal studies using rotating disk electrodes (RDE) allow transfer of kinetic and mass transport information to the operational environment of sensors developed from these materials. This is of particular advantage in the development of operational sensor devices from redox polymer modified electrodes.

Due to the unpredictable behavior of many polymer modified electrodes,⁴ the ability to precisely control the mass transport properties of redox polymers is difficult, although this is of great importance in the development of operational sensors. In a previous study, the mass and charge transport properties of $[\text{Os}(\text{bipy})_2(\text{PVP})_{10}\text{Cl}]\text{Cl}$ were found to be controlled by the type of contacting electrolyte employed.⁸ In perchloric acid, the polymer film was found to be dehydrated and compact due to electrostatic cross-linking; this resulted in zero permeability of the substrate $\text{Fe}(\text{III})$ due to physical exclusion. The mediated reduction reaction was consequently found to occur at the polymer/electrolyte interface. While in H_2SO_4 electrolyte, a more open polymer structure was evident due to protonation of the polymer backbone pyridine groups. This resulted in favorable substrate permeation and therefore through film electrocatalysis was observed. The ability to control the permeability of ion exchange redox polymers by the use of organic/aqueous-phase electrolytes has also been demonstrated.¹⁴ Both approaches are based on differences in polymer swelling in various solvents. Due to the general nature of the electrolyte/solvent interactions with the redox films, "fine control" of the mass transport properties of the polymer films is, however, impossible by these routes.

The desire to exert control over the mass/charge transport properties of the electroactive material is great. In order to exert greater control over these processes, the redox polymer $[\text{Os}(\text{bipy})_2(\text{PVP})_{10}\text{Cl}]\text{Cl}$ has been chemically cross-linked over the range 1-20 mol % cross-linking in a controlled fashion using the cross-linking agents *p*-dibromobenzene, 1,5-dibromopentane, and 1,10-dibromodecane. In this paper we report the effect of the chemical cross-linking on the mass/charge transport and electrocatalytic properties of the redox polymer $[\text{Os}(\text{bipy})_2(\text{PVP})_{10}\text{Cl}]\text{Cl}$ and demonstrate the novel measurement of coexisting electroactive substrates by utilizing the controlled mass transport through the polymer film.

EXPERIMENTAL SECTION

Materials and Reagents. The synthesis of $[\text{Os}(\text{bipy})_2(\text{PVP})_{10}\text{Cl}]\text{Cl}$ is described elsewhere.⁶ The molecular weight of

- (1) Murray, R. W. *Annu. Rev. Mater. Sci.* **1984**, *14*, 145.
- (2) Faulkner, L. R. *Chem. Eng. News* **1984**, *62* (Feb 27), 28.
- (3) Murray, R. W.; Ewing, A. G.; Durst, R. A. *Anal. Chem.* **1987**, *59*, 379A.
- (4) Oyama, N.; Anson, F. C. *Anal. Chem.* **1980**, *52*, 1192.
- (5) Turner Jones, E. T.; Faulkner, L. R. *J. Electroanal. Chem.* **1987**, *222*, 201.
- (6) Forster, R. J.; Vos, J. G. *Macromolecules* **1990**, *23*, 4372.
- (7) Forster, R. J.; Kelly, A. J.; Vos, J. G.; Lyons, M. E. G. *J. Electroanal. Chem.* **1989**, *270*, 365.
- (8) Forster, R. J.; Vos, J. G. *J. Chem. Soc., Faraday Trans.* **1991**, *87*, 1863.
- (9) Doherty, A. P.; Forster, R. J.; Smyth, M. R.; Vos, J. G. *Anal. Chem.* **1992**, *64*, 572.
- (10) Doherty, A. P.; Vos, J. G. *J. Chem. Soc., Faraday Trans.* **1992**, *88*, 2903.
- (11) Alberly, W. J.; Hillman, A. R. *Annu. Rep. Prog. Chem.* **1981**, *C78*, 377.
- (12) Andrieux, C. P.; Dumas-Bouchiat, J. M.; Saveant, J. M. *J. Electroanal. Chem.* **1982**, *131*, 1.
- (13) Doherty, A. P.; Forster, R. J.; Smyth, M. R.; Vos, J. G. *Anal. Chim. Acta* **1991**, *255*, 45.
- (14) Chen, X.; He, P.; Faulkner, L. R. *J. Electroanal. Chem.* **1987**, *222*, 223.

the PVP backbone as measured by viscometry was 600 000. The redox polymer was cross-linked directly on the electrode surface via the solid-state reaction with the cross-linking agents 1,5-dibromopentane, 1,10-dibromodecane, and *p*-dibromobenzene (Aldrich). Each cross-linking agent was used at levels of 1, 5, 10, and 20 mol % cross-linking. As the stoichiometry of the reaction is 2:1 this results in 2, 10, 20, and 40 mol % quaternization of the backbone pyridine groups. Coatings are obtained by mixing a controlled amount of a 1% (w/v) solution of the polymer in methanol with the appropriate amount of a methanol solution of the cross-linking agent, with subsequent drying at room temperature. Details of the cross-linking procedure will appear elsewhere.¹⁵ All solutions were prepared from water obtained from the Milli-Q water purification system; 0.1 mol dm⁻³ H₂SO₄ was used as the electrolyte throughout. Solutions of Fe(III) were prepared from reagent grade [(NH₄)Fe(SO₄)₂·12H₂O in 0.1 mol dm⁻³ H₂SO₄ electrolyte without further purification. NO₂⁻ solutions were prepared in 0.1 mol dm⁻³ Na₂SO₄. Mixed solutions of Fe(III) and NO₂⁻ were prepared by the addition of appropriate quantities of 0.1 mol dm⁻³ NO₂⁻ to Fe(III) solutions immediately prior to measurement. Current responses were corrected for dilution effects.

Procedures. *Cyclic Voltammetry, Rotating Disk Electrode Voltammetry, and Coulometry.* Cyclic voltammetry (CV) and RDE voltammetry were carried out using a conventional three-electrode electrochemical cell. The potentiostat used was the EG&G Princeton Applied Research Model 362 potentiostat, the rotating disk assembly was the Metrohm Model 629-10 RDE. Voltammograms were recorded on the Linseis Model 17100 X-Y recorder. All RDE experiments were carried out at a potential sweep rate of 5 mV s⁻¹. The reference electrode was the saturated calomel electrode (SCE). All potentials are quoted without regard to the liquid junction potential. The counter electrode was 1.0-cm² platinum gauze placed parallel to the working electrode at a distance of ≈1 cm. Coulometry was carried out using the EG&G Princeton Applied Research Model 379 digital coulometer placed in series between the working electrode and the potentiostat return. The charge due to the oxidation of Os(II) to Os(III) within the polymer film was measured during slow sweep rate CV (1.0 mV s⁻¹) from 0.0 to 0.6 V vs SCE. Results were corrected for background charging currents. All measurements were carried out at room temperature.

RESULTS AND DISCUSSION

Electrochemistry of Cross-Linked [Os(bipy)₂(PVP)₁₀Cl]Cl. Certain criteria for the cyclic voltammetric (CV) behavior of surface-immobilized redox species have been established, and this technique is useful in analyzing the electrochemical behavior of the immobilized electroactive material.¹⁶ The cyclic voltammetric behavior of [Os(bipy)₂(PVP)₁₀Cl]Cl cross-linked with *p*-dibromobenzene and 1,10-dibromodecane for all levels of cross-linking (i.e., 1, 5, 10, and 20 mol %) are similar. Certain features of the CV behavior are noteworthy. The effect of potential sweep rate on peak currents was found to be linear from 1.0 to 100 mV s⁻¹ for films of a thickness of 1 × 10⁻⁹ mol cm⁻². This indicates finite diffusional behavior operating up to 100 mV s⁻¹ with total consumption of the immobilized sites under the time scale of the measurements. This also suggests an absence of diffusional constraints on electrode currents. The onset of semiinfinite diffusional behavior due to redox site concentration polarization within the film occurs at potential sweep rates higher than 100 mV s⁻¹. The ratio of anodic to cathodic peak current (*i*_{pa}/*i*_{pc}) for both cross-linking agents was 1.0 ± 0.01 at all levels of cross-linking, indicating the kinetics of the forward and reverse processes are similar at all levels of cross-linking for *p*-dibromobenzene and 1,10-dibromodecane.

In addition, the peak width at half-height for both oxidation and reduction waves (fwhm) was found to be 90 ± 1 mV, in agreement with ideal surface behavior. Nernstian plots, for 20 mol % cross-linking with *p*-dibromobenzene and 1,10-dibromodecane, of log [Os(III)]/[Os(II)] vs applied electrode potential (*E*) were found to be linear over the range -2 ≤ log[Os(III)]/[Os(II)] ≤ 2 with a Nernstian slope of 58 ± 2 mV decade⁻¹. The operational potential [where log[Os(III)]/[Os(II)] = 1] was found to be 0.250 V vs SCE, in direct agreement with the CV estimated half-wave potential (*E*_{1/2}). These results indicate that the redox sites within the polymer are in thermodynamic equilibrium with the electrode potential and that the redox polymers possess sufficient void volume to accommodate incoming charge compensation counterions.¹⁷ These observations are directly comparable with the un-cross-linked material and are indicative of ideal surface behavior. It is evident that cross-linking with *p*-dibromobenzene and 1,10-dibromodecane does not result in altered electrochemical behavior of the electroactive sites. This is surprising as it has been shown previously that the electrochemical parameters of the electroactive centers in redox polymers are strongly dependent on the polymer matrix.¹⁸ It should be noted here that the redox polymers are only lightly cross-linked compared with electropolymerized materials or electrostatically cross-linked materials, so the redox site microenvironment may not be altered significantly by the levels of cross-linking used.

1,5-Dibromopentane cross-linked films exhibits similar CV behavior with some exceptions. The onset of semiinfinite diffusional behavior occurred at lower potential sweep rates (50 mV s⁻¹). Nernstian plots were found to be linear over the range -2 ≤ log[Os(III)]/[Os(II)] ≤ 1 with a slope of 57 ± 2 mV decade⁻¹. At greater than 50% oxidation, super-Nernstian responses were observed with slopes of 85 ± 3 mV decade⁻¹. These results indicate that, for this cross-linked agent, the redox sites are not in thermodynamic equilibrium with the electrode potential. It is believed that this is a result of insufficient polymer void volume to accommodate the counterion influx required to maintain electroneutrality. A theoretical model has recently been developed to couple the mechanical and electrochemical thermodynamics of redox polymer films on electrode surfaces.¹⁷ According to this theory, the super-Nernstian behavior is a result of the excess mechanical Gibbs free energy required for forced polymer swelling to accommodate the incoming counterions. Similar behavior has been observed for [Os(bipy)₂(PVP)₁₀Cl]Cl in perchloric acid electrolyte,⁸ plasma polymerized poly(vinylferrocene)¹⁹ (highly cross-linked), and linear poly(vinylferrocene)²⁰ in perchlorate electrolyte. This observation indicates that the polymer films cross-linked with 1,5-dibromopentane are more compact than those cross-linked with 1,10-dibromodecane and *p*-dibromobenzene. This is not surprising considering the small size of the C₅ cross-linking unit compared to the longer C₁₀ and the rigid *p*-dibromobenzene units.

Charge Transport Properties of Cross-Linked [Os(bipy)₂(PVP)₁₀Cl]Cl. In Figure 1 the charge transport diffusion coefficients (*D*_{ct}) for films cross-linked with each cross-linking agent and at each mole percent level are plotted. These values have been estimated by CV using the Randles-Sevcik equation under conditions of semiinfinite linear diffusion. Although there are inherent problems with such measurements, we believe that the diffusion coefficients obtained in this manner are more representative for the whole

(15) Doherty, A. P.; Vos, J. G. Submitted for publication in *Electroanalysis*.

(16) Hillman, A. R. In *Electrochemical Science and Technology of Polymers*; Linford, R. G., Ed.; Elsevier: Amsterdam, 1987; Vol. 1, Chapter 5.

(17) Bowden, E. F.; Dautartas, M. F.; Evans, J. F. J. *Electroanal. Chem.* 1987, 219, 49.

(18) Forster, R. J.; Vos, J. G. *Electrochim. Acta* 1992, 37, 159.

(19) Dautartas, M. F.; Bowden, E. F.; Evans, J. F. J. *Electroanal. Chem.* 1987, 219, 71.

(20) Bowden, E. F.; Dautartas, M. F.; Evans, J. F. J. *Electroanal. Chem.* 1987, 219, 91.

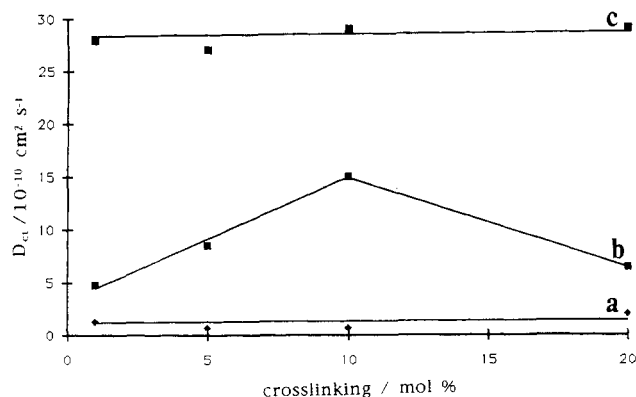


Figure 1. D_{ct} vs mole percent cross-linking for (a) *p*-dibromobenzene, (b) 1,5-dibromopentane, and (c) 1,10-dibromodecane cross-linked polymer. Values were estimated by high sweep rate CV in 0.1 mol dm^{-3} H_2SO_4 .

layer than those obtained by transient methods.^{7,8,18} Furthermore, the peak-to-peak separations obtained for these systems show Nernstian control in the scan rate range used, which allows such an analysis. The D_{ct} value for the uncross-linked material in 0.1 mol dm^{-3} H_2SO_4 is $1.8 \pm 0.2 \times 10^{-10} \text{ cm}^2 \text{ s}^{-1}$, which is comparable to that found previously.⁷ The D_{ct} values for polymer films cross-linked with *p*-dibromobenzene are similar and in the range $0.7 \pm 0.1 \times 10^{-10}$ to $2.0 \pm 0.2 \times 10^{-10} \text{ cm}^2 \text{ s}^{-1}$. These values are close to that found for the homopolymer. It appears that cross-linking with this reagent does not affect the charge transport rates of the polymer films significantly at any level of cross-linking. For 1,10-dibromodecane, the rate of charge transport was found to be constant at $2.8 \pm 0.1 \times 10^{-9} \text{ cm}^2 \text{ s}^{-1}$ between all levels of cross-linking. Again, no systematic trend in D_{ct} with level of cross-linking was observed. Surprisingly, the D_{ct} value for 1,10-dibromodecane is however ≈ 1 order of magnitude greater than for the homopolymer, indicating considerable improvements in the charge transport characteristics of the redox material. The D_{ct} values for the 1,5-dibromopentane cross-linked polymer films were found to increase from $4.8 \pm 0.3 \times 10^{-10}$ to $1.5 \pm 0.3 \times 10^{-9} \text{ cm}^2 \text{ s}^{-1}$ with increasing cross-linking from 1 to 10 mol %. At 20 mol % cross-linking, the D_{ct} value was found to decrease to $6.4 \pm 0.1 \times 10^{-10} \text{ cm}^2 \text{ s}^{-1}$. This is likely to be a result of ion transport constraints at the higher levels of cross-linking. These results demonstrate that it is possible to manipulate the physical properties of the redox polymer film by chemical cross-linking to exert control over charge transport rates without significantly affecting the thermodynamic behavior of the redox centers (vide supra). For the system studied here, the value for D_{ct} can be manipulated by cross-linking over the range $\approx 1.0 \times 10^{-10}$ to $\approx 3.0 \times 10^{-9} \text{ cm}^2 \text{ s}^{-1}$. The ability to control charge transport rates in this manner may be of great importance for the development of novel applications for these devices. Also, the fact that charge transport rates for *p*-dibromobenzene and 1,10-dibromodecane cross-linked films are independent of the level of cross-linking is of particular advantage as accurate levels of cross-linking are not critical to produce films of constant current carrying capacity. This may be important in the mass production of modified electrodes with constant charge transport properties.

The charge transport properties of $[\text{Os}(\text{bipy})_2(\text{PVP})_{10}\text{Cl}]\text{Cl}$ have been extensively studied, and the results obtained suggest that the overall rate of charge transport is most likely controlled by counterion motion.^{7,21,22} It has been observed that cross-linking of redox polymers results in compaction of

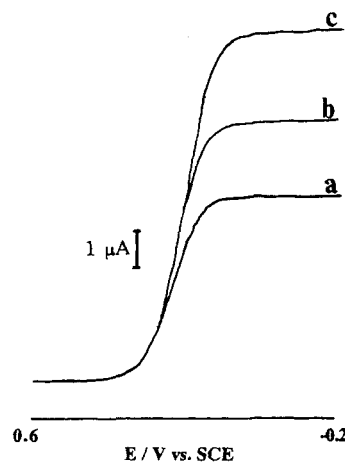


Figure 2. Typical RDE voltammograms for the mediated reduction of $1.0 \times 10^{-3} \text{ mol dm}^{-3}$ $\text{Fe}(\text{III})$ at a $1.0 \times 10^{-8} \text{ mol cm}^{-2}$ polymer film cross-linked with 10 mol % 1,10-dibromodecane: (a) 500, (b) 1000, and (c) 2500 rpm.

the polymer films, hindered short-range ion motion, and reduction in the current carrying capacity of the polymer films;²³ however, as the films studied here are lightly cross-linked, such effects may not occur. The increase in D_{ct} values observed may be explained by either of two effects resulting from cross-linking. First, contraction of the polymer film by cross-linking is likely to result in an increase in the effective redox site concentration (b_0) within the polymer film, resulting in a corresponding increase in values for D_{ct} . Alternatively, it is possible that crosslinking results in well-defined polymer morphology which facilitates counterion motion into the film upon oxidation. The reason for the increase in D_{ct} values is at present under detailed investigation.

Mediated Electrocatalysis at Cross-Linked $[\text{Os}(\text{bipy})_2(\text{PVP})_{10}\text{Cl}]\text{Cl}$. Detailed transport and kinetic models for electrocatalysis at redox polymer modified electrodes have been proposed.^{11,12} According to these models, the reaction of substrate at the redox polymer modified electrode can occur at any one of six possible reaction zones under 10 different transport or kinetically limiting processes. The reaction mechanism pertaining for a particular system is controlled by the relative importance of the following parameters: (a) the rate of charge transport through the polymer film (D_{ct}); (b) the extent of substrate partitioning into the film (K); (c) the diffusion of substrate within the film (D_s); (d) the rate of the cross-exchange reaction between substrate and mediator sites (k). As D_{ct} , K , D_s , and possibly k are directly influenced by the physical characteristics of the polymer film, it is therefore likely that cross-linking of the polymer will exert considerable influence over the transport and kinetic processes occurring during mediated electrocatalysis. In order to assess this, the mechanism for the mediated electrocatalytic reduction of $\text{Fe}(\text{III})$ at the cross-linked polymer films for each cross-linking agent and at each level of cross-linking was examined. In Figure 2, typical current-potential curves at various electrode rotation speeds for the mediated electrocatalytic reduction of $\text{Fe}(\text{III})$ at a 10 mol % 1,10-dibromodecane cross-linked film can be seen. These curves are well-defined with the onset of reduction occurring at the onset of $\text{Os}(\text{II})$ generation within the film, a clear demonstration of the electrocatalytic properties of the cross-linked redox polymer. In Figure 3, Levich plots for the mediated electrocatalytic reduction of $\text{Fe}(\text{III})$ at a modified electrode with surface coverage of $1.0 \times 10^{-9} \text{ mol cm}^{-2}$ are shown. Curves

(21) Forster, R. J.; Lyons, M. E. G.; Vos, J. G. *J. Chem. Soc., Faraday Trans. 1991*, 87, 3761.

(22) Forster, R. J.; Lyons, M. E. G.; Vos, J. G. *J. Chem. Soc., Faraday Trans. 1991*, 87, 3769.

(23) Oh, S. M.; Faulkner, L. R. *J. Electroanal. Chem.* 1989, 269, 77.

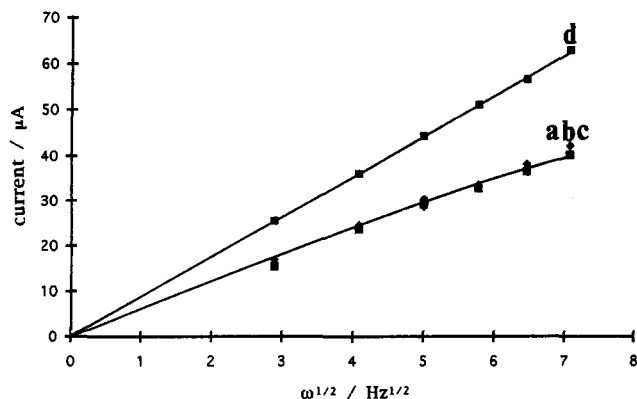


Figure 3. Levich plots for the reduction of $1.0 \times 10^{-3} \text{ mol dm}^{-3} \text{ Fe(III)}$ at a modified electrode cross-linked with 1,10-dibromodecane: (a) 5, (b) 10, and (c) 20 mol %; (d) theoretical Levich flux.

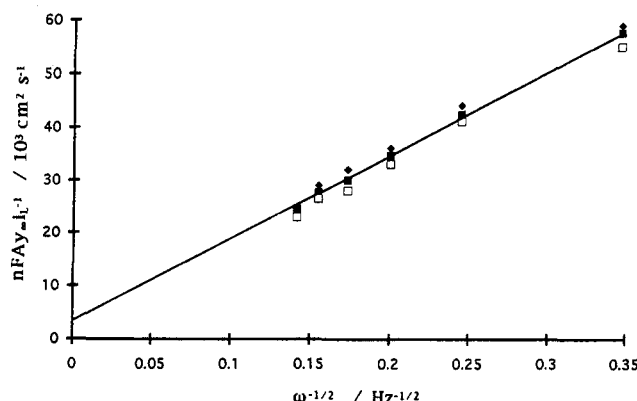


Figure 4. Koutecky-Levich plots for the reduction of $1.0 \times 10^{-3} \text{ mol dm}^{-3} \text{ Fe(III)}$ at modified electrodes cross-linked with 20 mol % 1,10-dibromodecane. Surface coverages: (■) 1.0×10^{-8} , (□) 1.0×10^{-9} , and (◆) $5.0 \times 10^{-10} \text{ mol cm}^{-2}$. The electrolyte was $0.1 \text{ mol dm}^{-3} \text{ H}_2\text{SO}_4$.

a-c represent the current flux as a function of electrode rotation speed for 5, 10, and 20 mol % cross-linking with 1,10-dibromodecane. Curve d shows the Levich flux. It is clear that the reaction flux at the modified electrode is considerably less than the Levich flux. This indicates that a chemical limitation step or transport-limiting processes control the electrode currents. Identical Levich behavior is observed for 1,5-dibromopentane cross-linked films at all levels of cross-linking. The corresponding Koutecky-Levich plots for a 20 mol % 1,10-dibromodecane cross-linked film at surface coverages of 1.0×10^{-8} , 1.0×10^{-9} and $5.0 \times 10^{-10} \text{ mol cm}^{-2}$ are shown in Figure 4. Identical plots were obtained at each level of cross-linking and also for 1,5-dibromopentane cross-linked films. In addition, current fluxes were similar for these cross-linking agents; this indicates that the kinetic situation for both cross-linking agents are the same. The diagnostic scheme of Albery et al.²⁴ can be used to elucidate the exact kinetic mechanism for both types of cross-linked films. The Koutecky-Levich plots are linear, and the currents are dependent on electrode rotation speed; the kinetic regimes St_e and LSt_e can therefore be eliminated from the 10 possible cases.²⁴ This is consistent with rapid charge transport within the polymer film. The inverse slope of the Koutecky-Levich plot is given by the Levich constant C_{Lev} :

$$C_{\text{Lev}} = 1.554D^{2/3}\nu^{-1/6} \quad (1)$$

where D is the diffusion coefficient of the substrate in solution and ν is the kinematic viscosity of the electrolyte. This value

has been estimated previously for clean unmodified electrodes to be $1.01 \times 10^{-3} \text{ cm s}^{-1/2}$.²⁴ The average Levich slope for all 1,10-dibromodecane cross-linked films was $9.1 \pm 0.8 \times 10^{-4}$ and $9.0 \pm 0.5 \times 10^{-4} \text{ cm s}^{-1/2}$ for 1,5-dibromopentane cross-linked films. These values are in close agreement with the unmodified electrode value and the value determined at un-cross-linked films ($9.4 \pm 0.8 \times 10^{-4} \text{ cm s}^{-1/2}$).⁸ This allows the elimination of the LRZt_e kinetic mechanism. It can be seen from the Koutecky-Levich plots that the magnitude of the modified electrode rate constant k'_{ME} (intercept of Koutecky-Levich plot) is independent of polymer layer thickness. This allows the elimination of the Lk and LEt_e kinetic cases. This leaves the Sk'' and LSk cases. These can be distinguished by the dependence of k'_{ME} on the concentration of electro-active sites within the film. Plots of $\ln k'_{\text{ME}}$ vs $\ln(1-f)$, where f is the fraction of redox sites in the oxidized state, were found to have a slope of 0.95 ± 0.04 . This indicates that the kinetic regime for both cross-linked films is Sk'' . In this situation the cross-exchange reaction occurs between redox sites in a region of polymer of molecular dimensions at the polymer/electrolyte interface. No partitioning of the substrate into the film occurs. The average value for k'_{ME} for both cross-linking agents is $2.0 \times 10^{-4} \text{ cm s}^{-1}$, the analytical expression for k'_{ME} under the Sk'' kinetic case is given by¹¹

$$k'_{\text{ME}} = k''b_o \quad (2)$$

where k'' is the second-order rate constant for the surface cross-exchange reaction. The magnitude of b_o estimated from the dry density of the polymer is $0.7 \times 10^{-3} \text{ mol cm}^{-3}$. This yields a value of $2.8 \pm 0.1 \times 10^{-4} \text{ mol}^{-1} \text{ dm}^3 \text{ cm s}^{-1}$ for the second-order rate constant k'' . This is in close agreement with the value obtained for the redox polymer in perchloric acid electrolyte, $3.1 \times 10^{-4} \text{ mol}^{-1} \text{ dm}^3 \text{ cm s}^{-1}$,⁸ where the polymer is highly electrostatically cross-linked by perchlorate ions. This confirms the surface nature of the reaction for 1,5-dibromopentane and 1,10-dibromodecane cross-linking agents.

The Sk'' kinetic case can arise in two situations: (a) when charge transport through the polymer and the rate of the cross-exchange reaction are so fast that the substrate flux is consumed without need for penetration of the polymer film; (b) where the substrate is physically unable to penetrate the polymer film. As the observed current flux is considerably less than the predicted Levich flux, it appears that the substrate is physically unable to penetrate the polymer film for both cross-linking agents at all levels of cross-linking. These observations can be quantified by estimating the characteristic currents defined by Saveant for (a) the cross-exchange reaction (i_k), (b) solution mass transport (i_a), and (c) electron transport (i_e).¹² These currents for the conditions used are given by the following equations:

$$i_k = nFAk''b_o y_s \quad (3)$$

$$i_a = nFADy_s/\delta_L \quad (4)$$

$$i_e = nFAD_{\text{ct}}\Gamma/L^2 \quad (5)$$

where n , F , and A have their usual meaning, y_s is the substrate concentration, δ_L is the diffusion layer thickness, Γ is the polymer surface coverage, D is the diffusion coefficient of Fe(III) in solution ($2 \times 10^{-6} \text{ cm}^2 \text{ s}^{-1}$), and L is the polymer layer thickness measured from the dry density of the polymer. For a D_{ct} value of $2.8 \times 10^{-9} \text{ cm}^2 \text{ s}^{-1}$ (for 1,10-dibromodecane) at a polymer surface coverage of $1.0 \times 10^{-8} \text{ mol cm}^{-2}$, the current i_e is 0.012 A cm^{-2} . The value for i_k at a substrate concentration of $1.0 \times 10^{-3} \text{ mol dm}^{-3}$ is $1.92 \times 10^{-5} \text{ A cm}^{-2}$. While i_a at an electrode rotation speed of 8.33 Hz, i_a is 0.033 A cm^{-2} . For total catalysis at the polymer surface, the conditions $i_k > i_a$ and $i_e > i_a$ must be satisfied. However, $i_a > i_k$, and $i_e > i_k$, so the electrode currents are under kinetic

(24) Albery, W. J.; Boutelle, M. G.; Hillman, A. R. *J. Electroanal. Chem.* 1985, 182, 99.

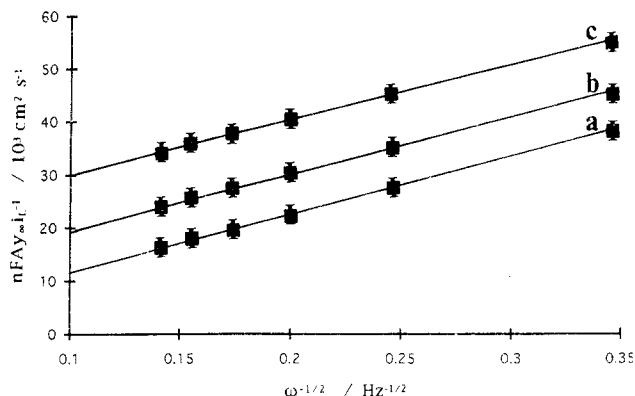


Figure 5. Koutecky-Levich plots for the reduction of 1.0×10^{-3} mol dm^{-3} Fe(III) at modified electrodes cross-linked with 1 (■) and 10 mol % (□) *p*-dibromobenzene. Surface coverages: (a) 1.0×10^{-8} , (b) 1.0×10^{-9} , and (c) 5.0×10^{-10} mol cm^{-2} . The electrolyte was 0.1 mol dm^{-3} H_2SO_4 .

control. Under these conditions the substrate flux is greater than the catalytic turnover at the polymer/electrolyte interface; therefore total consumption of the arriving substrate is impossible. If permeation of the polymer by the substrate is possible, the kinetic cases Lk or LSk would ensue from these conditions (vide infra).¹¹

For *p*-dibromobenzene cross-linked films, different mass transport behavior is observed. In Figure 5, Koutecky-Levich plots for the reduction of Fe(III) at surface coverages of 1.0×10^{-8} , 1.0×10^{-9} , and 5.0×10^{-10} mol cm^{-2} at 1 and 10 mol % cross-linking are shown. The behavior observed is clearly different from the dibromoalkane cross-linking agents (Figure 4). Again, the plots are linear and the currents are a function of electrode rotation speed. The average Levich slope is $1.4 \pm 0.2 \times 10^{-3}$ cm $\text{s}^{-1/2}$, which is close to the values cited earlier. These observations allow the elimination of the St_e , LSt_e , LEk , and LRZt_e kinetic cases. Plots of $\ln k'_{\text{ME}}$ vs $\ln L$ (where L is the polymer layer thickness) have a slope 1.1 ± 0.1 , showing a first-order relationship with respect to layer thickness. This indicates that the kinetic regime is Lk.²⁴ This suggests that Fe(III) penetrates the polymer film and that mediation occurs throughout the polymer with the rate constant for the cross-exchange reaction controlling limiting currents. The average value of k'_{ME} at the following film thickness is $L = 3.5$ nm, $k'_{\text{ME}} = 5.9 \times 10^{-5}$ cm s^{-1} ; $L = 7.5$ nm, $k'_{\text{ME}} = 1.2 \times 10^{-4}$ cm s^{-1} ; and $L = 35$ nm, $k'_{\text{ME}} = 6.7 \times 10^{-4}$ cm s^{-1} . The analytical expression for k'_{ME} under these conditions is given by

$$k'_{\text{ME}} = kKb_oL \quad (6)$$

where K is the substrate partition coefficient and k is the second-order rate constant for the Lk reaction. This yields a value of $2.5 \pm 0.2 \times 10^2$ mol $^{-1}$ dm 3 s $^{-1}$ for the apparent second-order rate constant kK . Assuming that the rate constant for the cross-exchange reaction is similar for the cross-linked polymer compared to the un-cross-linked material where $k = 2.8 \times 10^3$ mol $^{-1}$ dm 3 s $^{-1}$, the partition coefficient for the *p*-dibromobenzene cross-linked films can be estimated to be ≈ 0.1 . This value is approximately half of that obtained for the un-cross-linked material.⁸ This indicates increased mass transport restrictions due to cross-linking of the polymer film. This again can be quantified using the theory of Saveant.¹² The characteristic kinetic current for a through film reaction is given by the equation

$$i_k = nFAkKb_oL\gamma_s \quad (7)$$

This yields a value of 2.4×10^{-4} A cm $^{-2}$ for i_k at a surface coverage of 1.0×10^{-8} mol cm^{-2} , while the Levich current is 0.033 A cm $^{-2}$. As $i_k \ll i_a$, total consumption of the substrate

is therefore not obtained at this surface coverage. Total catalysis is achieved when the kinetic current equals the Levich flux ($\text{Lk} \rightarrow \text{LSk}$) and can be estimated from eq 7. The surface coverage required to effect total catalysis is 1.3×10^{-6} mol cm^{-2} . It should also be noted that the Koutecky-Levich plots are co-incident for each level of cross-linking, indicating that the partition coefficient is relatively insensitive to the level of cross-linking over the range 1–20 mol % for *p*-dibromobenzene, again, useful for the mass production of electrodes with identical properties.

From the transport data, it is evident that 1,5-dibromopentane and 1,10-dibromodecane cross-linked films inhibit permeation by the Fe(III) substrate at cross-linking levels as low as 1 mol %. The coincidence of the Koutecky-Levich plots for different levels of cross-linking plots is somewhat surprising considering the relatively open structure expected for a protonated/quaternized PVP backbone and the relatively ease of counterion incorporation. The impermeability may be related to the ionic radius of the $[\text{Fe}(\text{H}_2\text{O})_6]^{3+}$, known to be the predominant form of Fe(III) in acidic electrolyte. In addition, the driving force for incorporation of substrate and counterions is different; the partition of Fe(III) is concentration driven while counterion transport involves potential-driven active transport. For *p*-dibromobenzene films the ridged cross-linking agent allows permeation; this may be possible due to the ridged nature of the cross-linking agent, allowing some separation of the polymer chains on the electrode surface compared to the small C_5 residue and bond angle coiling of the C_{10} residues.

Electrochemical Measurement of Coexisting Electroactive Species. Due to the general nature of mediated electrocatalysis, great difficulty is encountered in controlling the selectivity of sensors developed from redox polymer modified electrodes. Isolation of the individual currents due to simultaneous electrode processes is impossible at conventional electrodes, while at previously described modified electrodes exclusion of the interfering species by charge or size discrimination is required.²⁵ Unfortunately, such exclusion is frequently incomplete and therefore some interference may be encountered;²⁵ in addition, the loss of additional analytical information concerning the excluded species is undesirable. In this section it will be demonstrated how the individual currents due to simultaneous reduction reactions of Fe(III) and NO_2^- at the modified electrode can be isolated by controlling substrate permeability and manipulating the polymer surface coverage, and how this can provide analytical information for both species.

The irreversible reduction of NO_2^- at $[\text{Os}(\text{bipy})_2(\text{PVP})_{10}\text{-Cl}]\text{Cl}$ modified electrodes has been demonstrated recently.¹⁰ The NO^+ species (as the ion-association complex $\text{HSO}_4^-\text{NO}^+$) is rapidly incorporated into the un-cross-linked polymer film with $K \approx 1$. At films cross-linked with 10 mol % 1,10-dibromodecane the value of K is reduced to ≈ 0.4 , indicating hindered mass transport; however, relatively facile incorporation is maintained along with relatively slow cross-exchange, resulting in through-film electrocatalysis (the Lk kinetic case).²⁶ At the same modified electrode, Fe(III) permeation is inhibited by size exclusion (vide supra). In order to isolate the individual currents for both electrode processes, the following conditions are assumed to prevail: (a) the reaction locus for NO_2^- reduction is throughout the entire polymer film (Lk) while confined to the polymer/solution interface for Fe(III) reduction (Sk''); (b) the kinetically controlled currents for both reduction processes are additive; (c) the current flux through the polymer is sufficient to maintain both reactions simultaneously. The first assumption is

(25) Wang, J.; Golden, T.; Tuzhi, P. *Anal. Chem.* **1987**, *59*, 740.

(26) Stanley, M. A.; Vos, J. G., unpublished results.

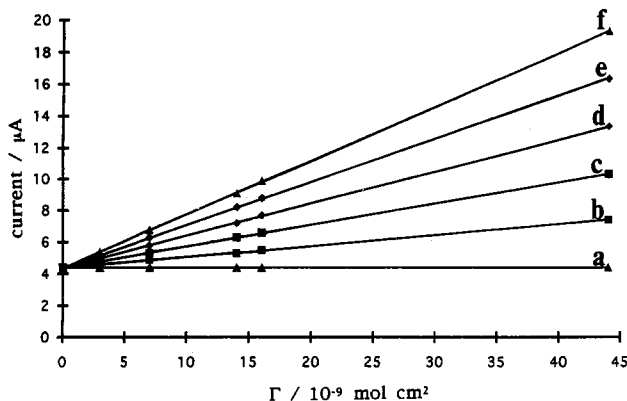


Figure 6. Electrode current vs film thickness for the reduction of (a) 2.0×10^{-4} mol dm $^{-3}$ Fe(III) with (b) 2.0×10^{-3} , (c) 4.0×10^{-3} , (d) 6.0×10^{-3} , (e) 8.0×10^{-3} , and (f) 1.0×10^{-2} mol dm $^{-3}$ NO $_2^-$ in 0.1 mol dm $^{-3}$ H $_2$ SO $_4$. The electrode rotation speed was 500 rpm.

implicit from the results described above while the supposition concerning the additive nature of electrode currents is proved later. The final assumption is verified by calculating the characteristic electron diffusion current i_e and comparing this with the combined characteristic kinetic currents for both electrode processes $i_{k(\text{total})}$. The value for i_e for the thickest polymer film used and for the D_{ct} value of 2.8×10^{-9} cm 2 s $^{-1}$ is 2.7×10^{-3} A cm 2 . The combined kinetic currents $i_{k(\text{total})}$ for both reactions at 5.0×10^{-3} mol dm $^{-3}$ Fe(III) and 1.0×10^{-2} mol dm $^{-3}$ NO $_2^-$ is 1.1×10^{-4} A cm $^{-2}$. As $i_e \gg i_{k(\text{total})}$, then the current carrying capacity of the film exceeds the catalytic capacity of the redox centers and the third assumption is verified.

In Figure 6, a plot of limiting current vs polymer surface coverage is shown for the reduction of Fe(III) at a concentration of 2.0×10^{-4} mol dm $^{-3}$ (Figure 6a) with various concentrations of NO $_2^-$ over the range 2.0×10^{-3} to 1.0×10^{-2} mol dm $^{-3}$ (figure 6b–f). It is evident that the plots are linear and by extrapolation to an infinitely small surface coverage (where surface coverage $\Gamma \rightarrow 0$ and the through-film reduction current for NO $_2^- \rightarrow 0$) have a common intercept of $4.4 \pm 0.1 \times 10^{-6}$ A. The value of the intercept current is equal to the limiting current for Fe(III) alone (Figure 6a). These plots can be described by a simple linear equation of the type $y = mx + c$, where y is the measured combined limiting current and c is the intercept current which corresponds to the current due to Fe(III) reduction and therefore the polymer/solution interface process. The term mx is the additional current due to reduction of NO $_2^-$ and the effect of increasing polymer film thickness on this Lk-type current. It is evident from these plots that the currents are additive for both electrode processes. In Figure 7, plots of current vs polymer surface coverage for a NO $_2^-$ concentration of 6.0×10^{-3} mol dm $^{-3}$ with varying Fe(III) concentration are shown. Again the plots are linear, with equal slopes as a result of NO $_2^-$ reduction; extrapolation to the intercepts ($\Gamma \rightarrow 0$) yields the current observed with Fe(III) alone. This demonstrates that the

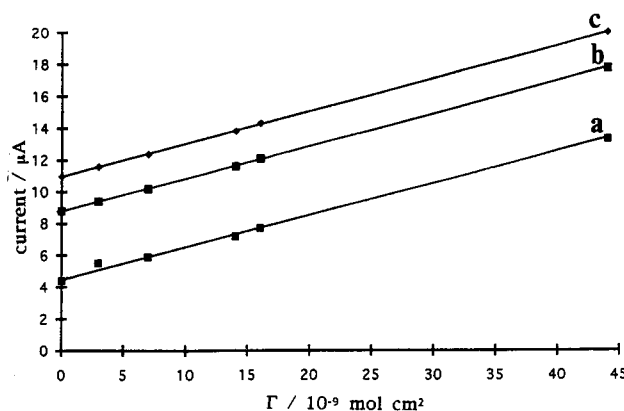


Figure 7. Electrode current vs film thickness for the reduction of 6.0×10^{-3} mol dm $^{-3}$ NO $_2^-$ with (a) 2.0×10^{-4} , (b) 4.0×10^{-4} , and (c) 5.0×10^{-4} mol dm $^{-3}$ Fe(III) in 0.1 mol dm $^{-3}$ H $_2$ SO $_4$. The electrode rotation speed was 500 rpm.

intercept current is a function of the Fe(III) reaction alone. Calibration of the individual electrode responses is now possible. The reaction order for the reduction of NO $_2^-$ is first order with respect to NO $_2^-$ concentration and polymer surface coverage,¹⁰ as expected from the theoretical model of Alberly and Hillman for purely outer-sphere electron transfer;¹¹ consequently, plots of slopes (of plots in Figure 6) vs NO $_2^-$ concentration are linear with zero-zero intercept. So, using a number of electrodes with various known surface coverages the analysis of the permeating (Lk) species can be accomplished. For Fe(III) calibration, plots of intercept current vs Fe(III) concentration are also linear, as expected from theory, with zero-zero intercept; again, such plots can be used for calibration purposes.

From these results it can be seen that isolation of the individual currents for two reactions occurring at the redox polymer modified electrode can be accomplished by control of the reaction loci for both species and by manipulation of the polymer surface coverage. This allows calibration for both responses and the ability to measure both species simultaneously, thus increasing the analytical information obtained concerning the system and also completely eliminating any interference due to the presence of the coexisting electroactive species. The extension of this approach to other systems, such as the simultaneous determination of dopamine and ascorbic acid, and multiple species determination using the finely tuned properties of the electroactive polymer films in electrode array devices, is at present under investigation.

ACKNOWLEDGMENT

The authors thank EOLAS (the Irish Science and Technology Agency) for financial assistance for this work.

RECEIVED for review May 27, 1993. Accepted August 27, 1993.*

* Abstract published in *Advance ACS Abstracts*, October 1, 1993.